Ex vivo HR-MAS MRS of human meningiomas: A comparison with *in vivo* ^{1}H MR spectra

VITALIANO TUGNOLI[1], LUISA SCHENETTI[2], ADELE MUCCI[2], FRANCESCA PARENTI[2], RITA CAGNOLI[2], VALERIA RIGHI[1,2], ANDREA TRINCHERO[1], LUCA NOCETTI[3], CRISTIAN TORACI[3], LUCIANO MAVILLA[4], GIANPAOLO TRENTINI[5], ELENA ZUNARELLI[5] and M. RAFFAELLA TOSI[6]

[1]Dipartimento di Biochimica 'G. Moruzzi', Università di Bologna, via Belmeloro 8/2, 40126 Bologna; [2]Dipartimento di Chimica, Università di Modena e Reggio Emilia, via G. Campi 183, 41100 Modena; [3]Struttura Complessa di Fisica Sanitaria, [4]Struttura Complessa di Neuroradiologia, Dipartimento di Neuroscienze, Testa e Collo, [5]Struttura Complessa di Anatomia Patologica, Azienda Ospedaliero-Universitaria di Modena-Policlinico, L.go del Pozzo 71, 41100 Modena; [6]ITOI/CNR, Sez. di Bologna, c/o IOR, via di Barbiano 1/10, 40136 Bologna, Italy

Received April 17, 2006; Accepted July 3, 2006

Abstract. We report on the magnetic resonance spectroscopy (MRS) characterisation of different human meningiomas. Three histological subtypes of meningiomas (meningothelial, fibrous and oncocytic) were analysed both through *in vivo* and *ex vivo* MRS experiments. The *ex vivo* high-resolution magic angle spinning (HR-MAS) investigations, permitting an accurate description of the metabolic profile, are very helpful for the assignment of the resonances *in vivo* of human meningiomas and for the validation of the quantification procedure of *in vivo* MR spectra. By using one- and two-dimensional experiments, we were able to identify several metabolites in different histological subtypes of meningiomas. Our spectroscopic data confirmed the presence of the typical metabolites of these benign neoplasms and, at the same time, that meningomas with different morphological characteristics have different metabolic profiles, particularly regarding macromolecules and lipids. The *ex vivo* spectra allowed a better understanding and interpretation of the *in vivo* MR spectra, showing that the HR-MAS MRS technique could be a complementary method to strongly support the *in vivo* MR spectroscopy and increase its clinical potentiality.

Correspondence to: Professor L. Schenetti, Dipartimento di Chimica, Università di Modena e Reggio Emilia, via G. Campi 183, 41100 Modena, Italy
E-mail: schene@unimo.it

Abbreviations: Ac, acetate; Ala, alanine; Asp, aspartate; Arg, arginine; CHESS, chemical shift selective saturation standard; Cho, choline; ChoCC, choline containing compounds; Chol, cholesterol; COSY, correlation spectroscopy; CPMG, Carr-Purcell-Meiboom-Gill; Cr, creatine; Cys, cysteine; 1D, one-dimensional; 2D, two-dimensional; E, ethanolamine; Glc, glucose; Gln, glutamine; Glu, glutamate; Glx, glutamine plus glutamate; Gly, glycine; GPC, glycerophosphocholine; GPE, glycerophosphoethanolamine; GSH, γ-glutamylcysteinylglycine, glutathione; His, histidine; HPF, high power field; HR-MAS, high-resolution magic angle spinning; HSQC, heteronuclear single quantum coherence; HTau, hypotaurine; Ile, isoleucine; LI, labelling index; Lac, lactate; Leu, leucine; Lip, lipids; Lys, lysine; MRS, magnetic resonance spectroscopy; Man, mannitol; Myo, *myo*-inositol; NAA, N-acetylaspartate; ß-OHBut, ß-hydroxybutyrate; PC, phosphocholine; PE, phosphoethanolamine; PEG, polyethylene glycol; Phe, phenylalanine; PRESS, point resolved spectroscopy; Pro, proline; Tau, taurine; Thr, threonine; TOCSY, total correlation spectroscopy; Tyr, tyrosine; UDP, uridine diphosphate; UMP, uridine monophosphate; Val, valine; VOI, volume of interest; WHO, World Health Organization

Key words: ex vivo HR-MAS MRS, *in vivo* MRS, meningiomas, metabolites, metabolomics, histopathological analysis

Introduction

The most frequent tumors of the central nervous system are represented by meningiomas. They typically manifest in adults and they are more common in women than in men. Meningiomas are generally slow-growing, benign tumors attached to the dura mater and composed of neoplastic meningothelial (arachnoidal) cells. Meningiomas have a wide range of histopathological appearances, among which meningothelial and fibrous are by far the most common. Moreover, 10-15% of meningiomas present an atypical pattern with rimlike enhancement, cyst formation, intralesion hemorrhage and metaplasia. Meningiomas with these morphological features resemble metastases or malignant gliomas with cystic or necrotic aspects (1). Although meningiomas have characteristic neuroimaging features, hemangiopericytomas, schwannomas, and dural metastatic tumors may mimic meningiomas (2).

Ex vivo HR-MAS MRS is a powerful analytical tool for human tissues by potentially bridging the divide between *in vitro* and *in vivo* MRS. The first applications of HR-MAS MRS on human tissue specimens date back to 1997 (3,4) and it has become possible thanks to the commercial diffusion of MRS probe-heads capable of studying the samples in rapid rotation around an axis at an angle of 54.7°

('magic angle') with respect to that of the static magnetic field. These probe-heads drastically reduce contributions from dipolar couplings, chemical shift anisotropy and susceptibility distortion providing high-resolution spectra from semi-solid samples such as tissues (5-12).

The quality of the obtained spectra is comparable to that from aqueous extracts, and the acquisition techniques that can be used are those employed in *in vitro* MRS, with the advantage of carrying out the measurements on intact tissue specimens without pre-treatment.

The purpose of this study was: i) to identify the metabolic patterns of meningiomas; ii) to assess the presence and the relevance of the metabolic alterations linked to different subtypes of meningiomas; iii) to compare the *ex vivo* and the *in vivo* spectra to clarify and validate the *in vivo* MRS.

Materials and methods

This study was approved by the local ethics committee and the patients provided a written informed consent. Six patients underwent surgical resection of the tumors and the specimens were snap-frozen in liquid nitrogen and stored at -80˚C until *ex vivo* MRS analysis.

Histopathological analysis of the 6 lesions identified them as meningiomatous in nature. According to the WHO 2000 criteria (13), three out of the six meningiomas were classified as classic meningothelial, grade I, one as classic fibrous, grade I, and one as classic transitional, grade I. One of them showed oncocytic differentiation, demonstrated both by conventional histology and immunohistochemistry (14). The neoplastic cells showed prominent nucleoli and focally high nucleus/cytoplasm ratio. The mean mitotic index (total counts per ten high-power fields) was 6/10 HPF, increasing up to 12/10 HPF in some areas. The lesion was therefore classified as grade II. The cellular proliferation index, determined by MIB-1, and expressed as LI, ranged from 1-3% for 4 meningiomas of the meningothelial, transitional and fibrous subtypes, consistent with grade I lesions. In one meningioma of the meningothelial subtype MIB-1 LI was slightly increased to 5%, but was still in keeping with a grade I lesion. The MIB-1 LI for the oncocytic meningioma was much higher; its mean value was 5%, and approached 14% in some areas, thus classified as a grade II lesion. The clinical data and MRS experiment types of the 6 patients are shown in Table I.

In vivo [1]H MRS. The patients underwent MRI and *in vivo* ^{1}H MRS of the head on a 3T clinical imager (Philips Intera, Best, The Netherlands).

I*n vivo* ^{1}H MR spectra were performed using a spin-echo sequence with 38 and 144 ms TE, 2s TR, 2048 data points, point resolved spectroscopy (PRESS) localisation technique and averaging the signal of 128 scans. The VOIs (6-8 cm^3) were placed and shaped according to the size of the lesion. Water signal suppression was performed using a chemical shift selective saturation standard (CHESS) sequence with two Gaussian chemical shift selective pulses of 70 Hz. The data were processed and analyzed using software developed by one of the authors (C.T.) on IDL platform (Research System, Inc., Boulder, CO, USA). DC correction, zero filling

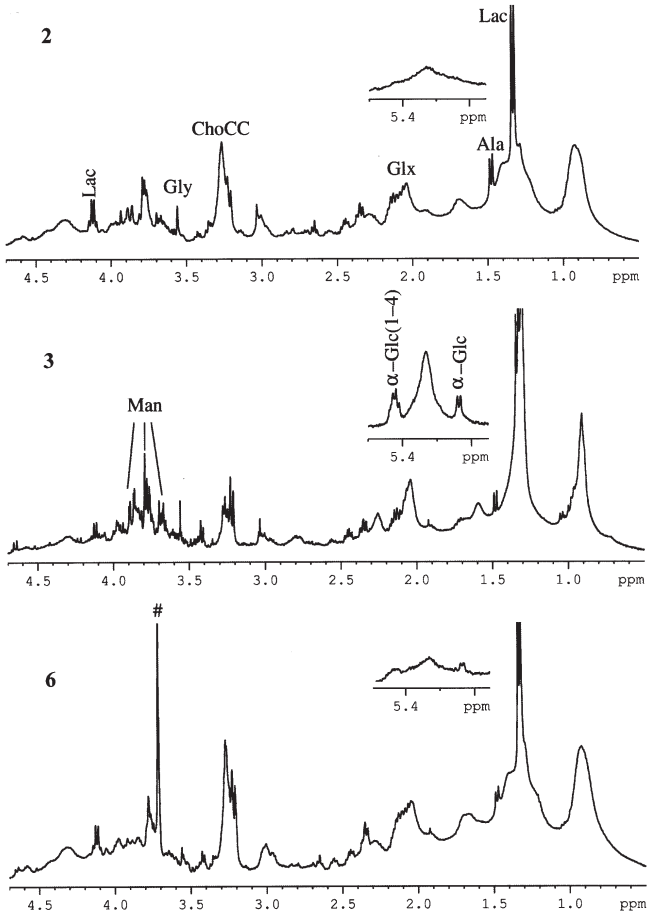

Figure 1. *Ex vivo* 1D ^{1}H conventional presaturated HR-MAS MR spectra of samples: 2, meningothelial; 3, fibrous; and 6, transitional. #, denotes PEG.

factor 2, Gaussian filter with LB 3.0 Hz (time domain), high pass filter bandwith 50 Hz (to suppress water peak) and baseline correction were applied to the spectral data.

Ex vivo HR-MAS MRS. Before MRS examination, each sample was flushed with D_2O with the aim to improve the homogeneity, the water suppression, and to add deuterium as a nucleus for the lock system. The sample was introduced in a MAS zirconia rotor (4 mm OD), fitted with a 50 μl cylindrical insert to increase sample homogeneity, and then transferred into the probe cooled to 4 ˚C.

^{1}H and ^{13}C HR-MAS spectra were recorded with a Bruker Avance400 spectrometer operating at a frequency of 400.13 and 100.61 MHz, respectively. The instrument was equipped with a ^{1}H,^{13}C HR-MAS probe. Experiments were performed at a temperature of 4˚C controlled by a Bruker cooling unit. Samples were spun at 4000 Hz and three different types of one-dimensional (1D) proton spectra were acquired by using the sequences implemented in the Bruker software: i) a composite pulse sequence (zgcppr) (15) with 1.5 s water presaturation during the relaxation delay, 8 kHz spectral width, 32k data points, 32 scans, ii) a water-suppressed spin-echo Carr-Purcell-Meiboom-Gill (CPMG) sequence (cpmgpr) (16) with 1.5 s water presaturation during the relaxation delay, 1 ms echo time (τ) and 360 ms total spin-

Table I. Patients' clinical data and NMR experiments.

Patient	Age (sex)	Meningioma Subtype and grade MIB-1 LI (%)	*In vivo* ^{1}H-MRS		*Ex vivo* HR-MAS MRS		
			TE 38 ms	TE 144 ms	1D ^{1}H zgcppr	1D ^{1}H cpmgpr	1D ^{1}H led
1	66 (M)	Meningothelial, grade I MIB-1 LI 1%			1a	1b	1c
2	53 (F)	Meningothelial, grade I MIB-1 LI 3%	X	X	2a	2b	2c
3	61 (F)	Fibrous, grade I MIB-1 LI 1%	X	X	3a	3b	3c
4	26 (M)	Oncocytic, grade II MIB-1 LI 5%, up to 14%	X	X	-	-	-
5	50 (F)	Meningothelial, grade I MIB-1 LI 5%	X	X	5a	5b	5c
6	74 (M)	Transitional, grade I MIB-1 LI 2%			6a	6b	6c

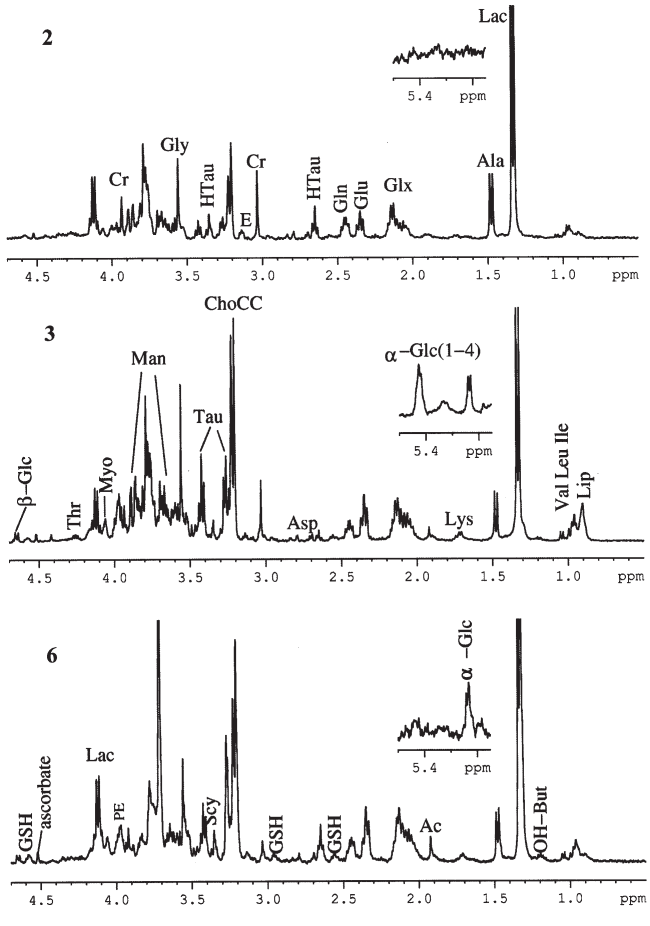

Figure 2. *Ex vivo* CPMG spectra of samples 2, 3 and 6 obtained with a 360 ms total spin-echo time.

spin relaxation delay (2nτ), 8 kHz spectral width, 32k data points, 256 scans and iii) a sequence for diffusion measurements based on stimulated echo and bipolar-gradient pulses (ledbpgp2s1d) (17) with big delta 200 ms, eddy current delay T_e 5 ms, little delta 2x2 ms, sine-shaped gradient with 32 G/cm followed by a 200 μs delay for gradient recovery, 8 kHz spectral width, 8k data points, 256 scans.

Two-dimensional (2D) ^{1}H,^{1}H-correlation spectroscopy (COSY) (18,19) spectra were acquired using a standard pulse sequence (cosygpprqf) and 0.5 s water presaturation during relaxation delay, 8 kHz spectral width, 4k data points, 32 scans per increment, 256 increments. 2D ^{1}H,^{1}H-total correlation spectroscopy (TOCSY) (20,21) spectra were acquired using a standard pulse sequence (mlevphpr) and 1 s water presaturation during relaxation delay, 100 ms mixing time (spin-lock), 4 kHz spectral width, 4k data points, 32 scans per increment, 128 increments. 2D ^{1}H,^{13}C-heteronuclear single quantum coherence (HSQC) (22) spectra were acquired using an echo-antiecho phase-sensitive standard pulse sequence (hsqcetgp) and 0.5 s relaxation delay, 1.725 ms evolution time, 4 kHz spectral width in f2, 4k data points, 128 scans per increment, 17 kHz spectral width in f1, 256 increments.

Results and Discussion

HR-MAS spectra. Fig. 1 shows the *ex vivo* 1D ^{1}H conventional HR-MAS MR spectra of three subtypes of meningiomas diagnosed as meningothelial (patient 2), fibrous (patient 3) and transitional (patient 6). The spectra

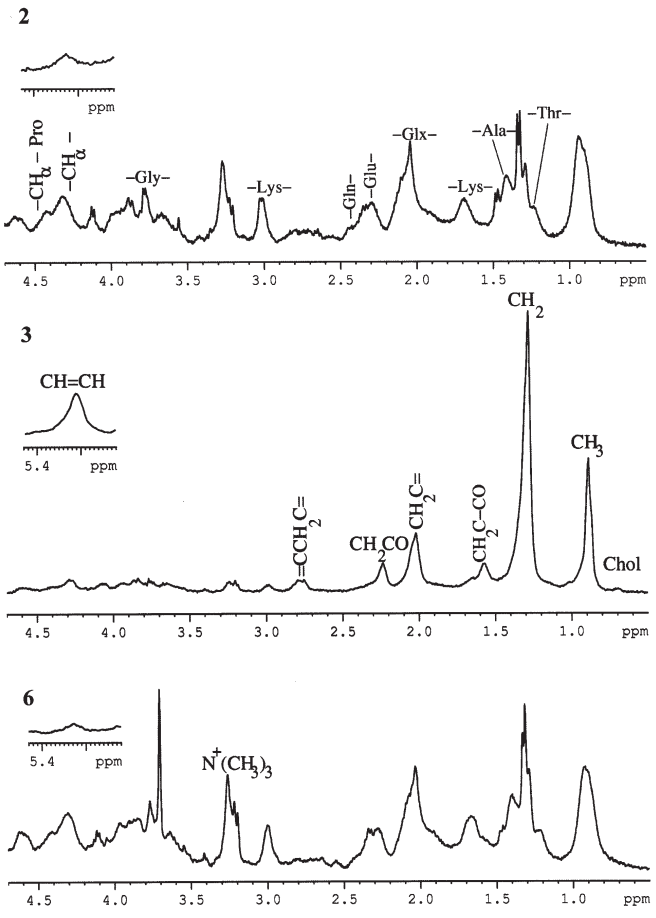

Figure 3. *Ex vivo* diffusion-edited spectra of samples 2, 3 and 6 obtained with Δ=200 ms, δ=4 ms and a gradient strength of 32 G/cm.

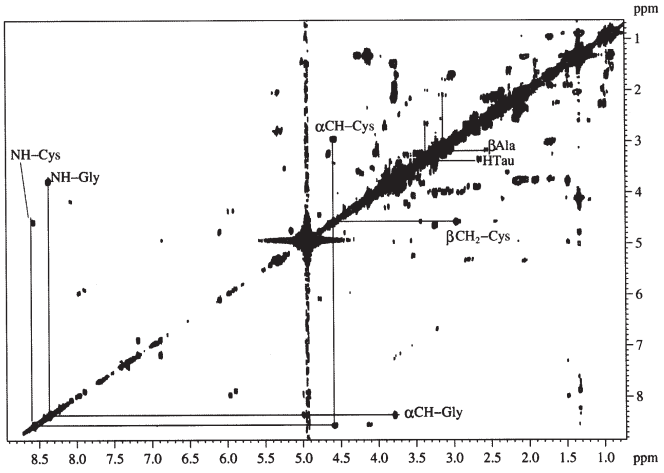

Figure 4. COSY spectrum of sample 1.

highlight both narrow and broad signals, which can be separated by using a CPMG spin-echo and a diffusion-edited sequence. Fig. 2 shows the spin-echo spectrum displaying signals due to the resonances of small metabolites, and Fig. 3 displays the diffusion-edited spectrum in which contributions from mobile lipids and macromolecules were found. The labels were chosen to indicate the more abundant and visible metabolites (Figs. 1 and 2) and macromolecules (Fig. 3) in each spectrum.

The efficacy of the above sequences at clarifying tissue components is remarkable when considering the region at ~3.2 ppm, which is of great importance in *in vivo* spectroscopy, because it contains signals due to ChoCC. This region, as is particularly evident in samples 2 and 6 (Fig. 1), is formed by overlapping broad and narrow signals. In the CPMG experiment (Fig. 2) the narrow signals due to Cho, GPC, PC, Tau, and a low percentage Myo, are highlighted, whereas the broad component due to the $N^+(CH_3)_3$ of phospholipids is evident in the diffusion-edited spectrum (Fig. 3).

The detection of metabolites was obtained, not only through 1D ^{1}H MRS spectra, but also through selected 2D experiments such as COSY, TOCSY and HSQC, and their assignment was confirmed by comparison with literature data. COSY and TOCSY spectra were very informative for the identification of hidden resonances: COSY spectra enabled coupled proton-proton pairs to be found, whereas the TOCSY spectra permitted ^{1}H,^{1}H connectivities of up to five or six bonds and metabolite spin systems to be identified. HSQC spectra revealed directly bonded carbon-proton pairs, thus enabling the assignment of singlets (which do not give correlations in homonuclear COSY and TOCSY spectra), and the discrimination among compounds having similar proton but diverse ^{13}C chemical shifts. The full experiments provided complete and unambiguous identification of the metabolic pattern characterising the examined tissues. The main metabolites are labeled in Figs. 1-6 and the pool of metabolites especially osmolites, free amino acids and mobile lipids are reported in Table II.

Low molecular-weight metabolites. Abundant metabolites such as Lac, Ala, Glu, Gln, Cr, ChoCC, Tau and Gly can be identified by direct inspection of the 1D ^{1}H MRS spectra obtained using the spin-echo sequence, whereas, the identification of metabolites hidden under the more abundant ones can be obtained through COSY, TOCSY and HSQC spectra. For example, the presence of the GSH, particularly abundant in sample 1, was established by the COSY cross-peaks between the signals at 8.57 and 8.36 ppm with signals at 4.57 and 3.77 ppm, respectively (Fig. 4). These correlations are attributed to the NH/CH(α) pair of Cys and NH/CH_2 of Gly in GSH and their detection indicates that the NH protons of glycyl and cysteinyl amidic groups are in slow-exchange with water. This assignment was confirmed by a TOCSY spectrum (showing a further correlation between NH at 8.57 ppm and CH_2 at 2.96 ppm of Cys), and by the HSQC spectrum, showing the H,C correlation at 3.77/44.0 ppm, attributable to the CH_2 group of a bonded Gly, clearly distinguishable from free Gly, whose H,C correlation is found at 3.56/42.3 ppm (Fig. 6). It is also to be noted that the resonances of the glutamyl moiety of GSH were well distinguished from those of free Gln and Glu (Fig. 5, left). The other resonances due to cysteinyl and glutamyl moieties of GSH are reported in Table II.

HTau was identified by the triplet at 2.65 ppm, which correlated with a triplet at 3.35 ppm in the COSY spectrum,

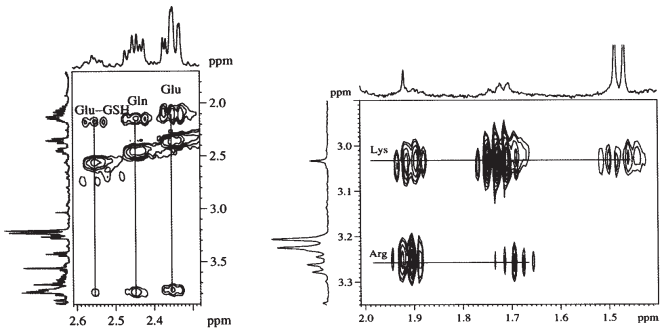

Figure 5. Partial TOCSY spectra of sample 1 (left) and sample 3 (right).

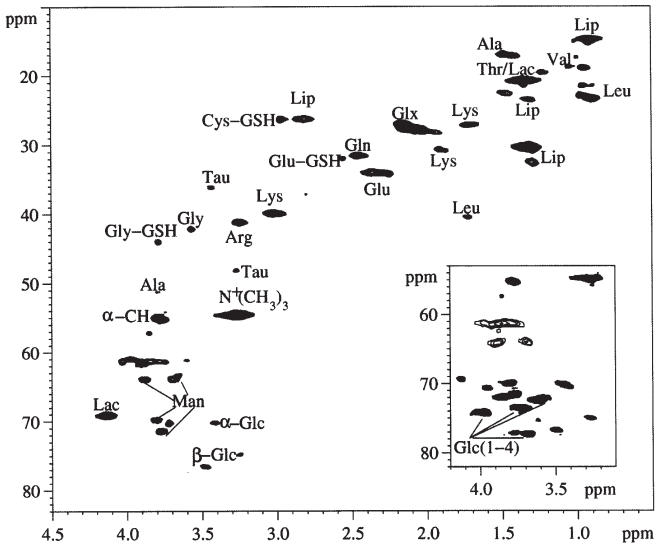

Figure 6. HSQC spectrum of sample 1. The insert shows a selected region of sample 3.

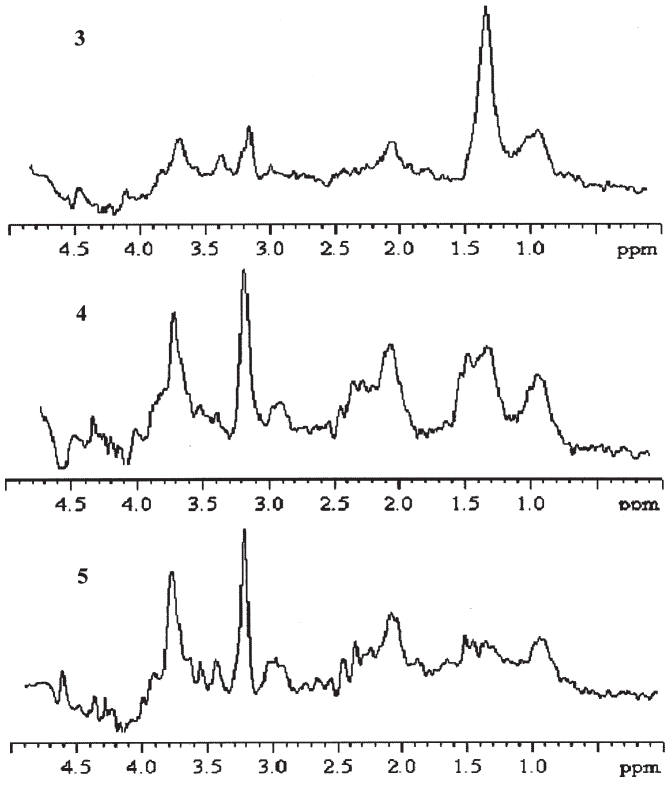

Figure 7. *In vivo* MR spectra of meningiomas 3, fibrous; 4, oncocytic; and 5, meningothelial recorded at 3 T with TE=38 ms.

whereas ß-Ala, which is the major product of uracil catabolism (23), displayed a correlation between a triplet at 2.55 ppm and a triplet at 3.18 ppm.

The resonances of the methyl groups of Leu, Ile, Val were in the range between 0.94-1.04 ppm and appeared, in 1D ^{1}H spectra, as a shoulder of a broad band at 0.9 ppm due to methyl resonances of lipids and macromolecules. The identification of these amino acids was easily obtained through the COSY and TOCSY spectra. Val was identified by the correlation between the methyl resonances at 0.99 and 1.04 ppm with the ß-CH at 2.25 ppm. Ile was characterised by the resonances at 1.02 ppm and 1.97 ppm, and Leu was identified by the correlations between the signals at 0.95 and 0.97 ppm with that at 1.72 ppm. The signals of Lys, more evident in sample 3, and Arg were partially overlapped with those of Leu and Ile; their clear identification was achieved, from COSY spectra, by the correlations at 3.02/1.73 ppm for Lys and at 3.23/1.70 ppm for Arg. Further confirmation came from the correlations in the TOCSY spectra (Fig. 5, right). The same 2D homonuclear experiments revealed the methyl doublet of Thr at 1.33 ppm (hidden in all samples under that of Lac) by its correlation with α-CH at 4.26 ppm.

The region of the ^{1}H spectra at around 3.2 ppm, which displayed resonances usually attributed to ChoCC (GPC, PC and Cho) in the *in vivo* spectra, received contributions, in the reported samples, from PE, Myo, ß-Glc, Tau, Arg and GPE, as already observed in a previous study (8). Regarding ChoCC, Cho and PC were the main metabolites, whereas GPC was not detected. In all meningiomas, traces of ascorbate (a doublet at 4.52 ppm correlating with a signal at 4.01 ppm), aromatic metabolites such as Phe, adenosine, uracil, UMP, UDP, Tyr, His and fumarate were found in varying percentages.

Samples 1 and 6 were the richest ones in GSH, whereas it was present only at trace level in samples 3 and 5. GSH is expected to be present in meningiomas, but it is difficult to find in extracts (2,24). The detection of GSH in tumoral tissues is important in relation to its documented tumor chemoresistance (25,26,27). Moreover, GSH is metabolically linked to Ala, Gln and Glu (24) and this correlation probably indicates why these metabolites are present in appreciable amounts in the meningiomas studied. GSH participates in many cellular reactions and its metabolism is implicated for health (28) and with respect to cancer, it is able to play both protective and pathogenic roles (25).

The presence of HTau together with Tau is probably due to the redox balance in these metabolites; indeed HTau is a precursor of Tau, the main end product of Cys metabolism in mammals, and is thought to share the same physiological function (29). Tau is the most abundant amino acid found in the mammalian brain and seems to play a role in a wide

Table II. The ^{1}H and ^{13}C chemical shifts (δ, ppm) of metabolites found in HR-MAS spectra of meningiomas.[a,b]

Entry	Metabolite	δ ^{1}H	δ ^{13}C	Assignment
1	Fatty acids	0.89	14.6	CH_3
		1.29-1.31	29.8-32.0	$(CH_2)_n$
		1.59-1.60	25.2	CH_2-C-C=O
		2.02	27.8	CH_2-C=
		2.24	34.2	CH_2-C=O
		2.78	26.2	=C-CH_2-C=
		5.32	130.2; 128.4	CH=CH
2	Cholesterol	0.70		CH_3
		0.92		CH_3
3	Isoleucine	0.94 (t)		δ-CH_3
		1.02 (d)	15.5	γ-CH_3
		1.97		γ-CH_2
				ß-CH
				α-CH
4	Leucine	0.95 (d)	21.5	δ-CH_3
		0.97 (d)	22.8	δ-CH_3
		1.70		γ-CH
		1.72	40.4	ß-CH_2
		3.75	c	α-CH
5	Valine	0.99 (d)	17.3	γ-CH_3
		1.04 (d)	18.7	γ-CH_3
		2.25		ß-CH
		3.61	61.2	α-CH
6	ß-OH-butyrate	1.18 (d)		γ-CH_3
		4.14		ß-CH
7	Threonine	1.33 (d)	20.3	γ-CH_3
		4.26	66.6	ß-CH
		3.60	61.2	α-CH
8	Lactate	1.33 (d)	20.3	CH_3
		4.11	61.9	CH
9	Alanine	1.48 (d)	16.8	ß-CH_3
		3.78	51.1	α-CH
10	Acetate	1.92	24.8	CH_3
11	ß-Alanine	3.18		ß-CH_2
		2.56		α-CH_2
12	Glutamate	2.35 (t)	34.0	γ-CH_2
		2.06, 2.14	27.9	ß-CH_2
		3.77	c	α-CH
13	Glutamine	2.44 (td)	31.5	γ-CH_2
		2.14	27.2	ß-CH_2
		3.78	c	α-CH
14	Glutathione	2.55	31.8	γ-CH_2 Glu
		2.16		ß-CH_2 Glu
		3.80	c	α-CH Glu
		2.96	26.3	ß-CH_2 Cys
		4.57	56.1	α-CH Cys
		3.77	44.0	CH_2 Gly
		8.57		NHCys
		8.36		NH Gly
15	Hypotaurine	2.65(t)		NCH_2
		3.35(t)		SCH_2
16	Aspartate	2.68, 2.82	37.2	ß-CH_2
		3.90		α-CH
17	Asparagine	2.85, 2.96	26.3	ß-CH_2
		4.01		α-CH

Table II. Continued.

Entry	Metabolite	δ ^{1}H	δ ^{13}C	Assignment
18	Creatine	3.04 (s)		NCH_3
		3.92(s)		NCH_2
19	Lysine	3.02(t)	39.9	ε-CH_2
		1.71	27.1	δ-CH_2
		1.48	22.5	γ-CH_2
		1.91	30.6	ß-CH_2
		3.79	c	α-CH
20	Arginine	3.23	41.3	δ-CH_2
		1.69		γ-CH_2
		1.92	28.1	ß-CH_2
		3.78	c	α-CH
21	Ethanolamine	3.15 (t)		NCH_2
		3.82 (t)		OCH_2
22	Phospho-ethanolamine	3.23	41.1	NCH_2
		4.01	61.1	OCH_2
23	Glycerophospho-ethanolamine	3.31		NCH_2
		4.10		OCH_2
24	free Choline	3.20	54.6	$N(CH_3)_3$
		3.53	68.2	NCH_2
		4.08	56.5	OCH_2
25	Phosphocholine	3.22	54.7	$N(CH_3)_3$
		3.61	67.3	NCH_2
		4.22	59.0	OCH_2
26	Glycine	3.56	42.3	CH_2
27	ß-Glucose	4.65 (d)	96.6	1-CH
		3.26	74.8	2-CH
		3.40	70.0	4-CH
		3.48	76.6	3,5-CH
28	Taurine	3.26(t)	48.1	SCH_2
		3.42(t)	35.9	NCH_2
29	*Myo*-inositol	3.53(dd)	72.0	1,3-CH
		4.06(t)		2-CH
		3.30(t)	73.1	5-CH
		3.63(t)		4,6-CH
30	*Scyllo*-inositol	3.35(s)	73.9	CH
31	α-Glucose	5.24(d)	92.6	1-CH
		3.54	72.0	2-CH
		3.73	73.8	3-CH
		3.42	70.0	4-CH
		3.88	72.5	5-CH
32	α-Glu-(1→4)	5.39, 5.41	100.2	1-CH
		3.62	72.2	2-CH
		3.98	74.0	3-CH
		3.68	77.2	4-CH
		3.73	73.5	5-CH
33	Serine	3.96	61.2	ß-CH_2
		3.84	57.0	α-CH
34	Ascorbate	4.52(d)		4-CH
		4.01		5-CH
35	Glyerol (in lipids)	4.10, 4.30	62.1	1,3-CH_2
		5.26	69.2	2-CH
36	Gycerol	3.56, 3.65	63.3	1-CH_2
		3.81	72.7	2-CH

Table II. Continued.

Entry	Metabolite	δ ^{1}H	δ ^{13}C	Assignment
37	UDP	5.92		1-CHrib
		4.35		2-CHrib
		5.90 (d)		5-CHur
		7.89 (d)		6-CHur
38	Uracil	5.80 (d)		5-CHur
		7.54 (d)		6-CHur
39	UMP	5.98		1-CHrib
		4.37		2-CHrib
		5.97 (d)		5-CHur
		8.11 (d)		6-CHur
40	Fumarate	6.52		CH
41	Tyrosine	3.06, 3.20		ß-CH_2
		3.93	56.7	α-CH
		7.23	131.5	2,6-H
		6.89	116.5	3,5-H
42	Histidine	7.85 (s)		2-CH
		7.08 (s)		4-CH
43	Phenlyalanine	3.11, 3.28		ß-CH_2
		3.99		α-CH
		7.34	130.1	2,6-H
		7.44	129.6	3,5-H
		7.37		4-H
44	Adenosine	8.36		2-CH
		8.23		8-CH
		6.10		1' -CH
		4.77		2' -CH
		4.43		3' -CH

[a,1]H chemical shifts refer to Ala doublet at 1.48 ppm; [b,13]C chemical shifts refer to Ala at 16.8 ppm; c, Ca probably contributes to the 3.77, 55.1 ppm cross peak.

range of basic physiological functions (30). The presence of these metabolites with antioxidant activity (GSH and HTau) needs further investigation, performed by multidisciplinary analytical approaches, to gain new insight into the redox state in neoplastic tissues.

It is worth noting that the *ex vivo* 1D and 2D ^{1}H MRS experiments showed the absence of N-acetylaspartate (NAA) in all the examined samples, in accordance with the extracerebral origin of these lesions.

Table III shows the integral ratios with respect to Ala=1 of the main metabolites detected in *ex vivo* CPMG spectra; Ala was chosen since it is a well-known metabolite characteristic of meningiomas (31). It should be noted that Ala intracellular level is intrinsic to the identity of the meningeal cell type and it is maintained through neoplastic transformation (32). The high amount of Ala in human meningiomas can be explained in light of this connection.

Glu plus Gln (Glx), free Cho, ChoCC, Ala, Gly, and Tau are known to be the main components of meningiomas together with relatively low amounts of Cr, as derived by the high Ala/Cr ratio typical of meningiomas (33).

Lipids and macromolecules. The most significant differences among the meningiomas appear to be in the large components of 1D ^{1}H presaturated (Fig. 1) and in 1D ^{1}H diffusion-based MR spectra (Fig. 3).

The profiles of samples 2 and 3 represent two limit situations. Sample 2 displays large components due to phospholipids (identified by the signals of $N^{+}(CH_3)_3$ at 3.23/54.8 ppm) and mobile peptidic residues. The amino acidic components of these residues were found from the resonances of bonded amino acids CH-α (broad signal centered at 4.35 ppm) (34) and their correlations with the relevant protons. An accurate analysis of TOCSY and HSQC spectra permitted the following amino acids to be found: Thr (1.22 ppm), Ala (1.41/17.1 ppm), Lys (3.02, 1.80 and 1.68 ppm), Glx (2.50÷2.20, and 2.10 ppm), Gly (3.92/43.5 ppm) and proline (Pro) (4.44/61.2 ppm, 2.28 ppm). A similar profile is displayed by sample 5 (meningothelial) and sample 6, identified by the histopathological analysis as transitional.

The profile of sample 3 is characterised by the dominant resonances of triglycerides and by a trace of cholesterol (Chol) (identified by the methyl resonances at 1.04 and 0.73 ppm). The analysis of the spectrum showed that the triglycerides were formed by saturated, mono- and poly-unsaturated fatty acids. Unsaturated acids were identified by the signals at 5.33 ppm, due to the ethylenic protons, and by the signals at 2.02 ppm, due to the methylenic protons of the

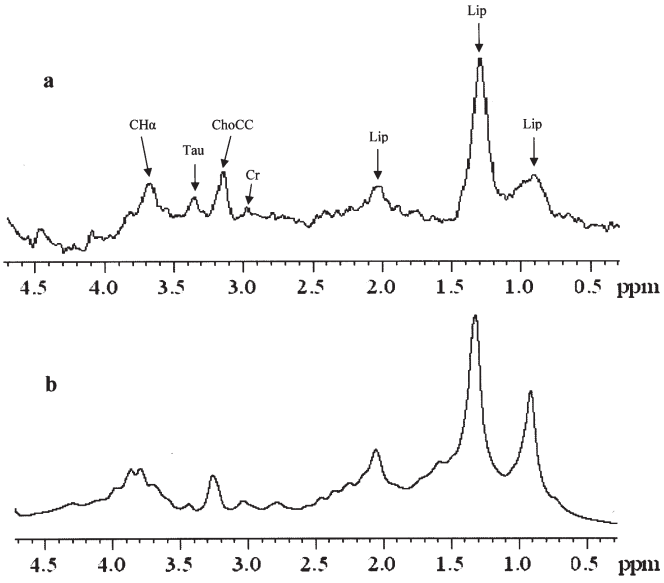

Figure 8. *In vivo* (a) (TE = 38 ms) and *ex vivo* (b) MR spectra of sample 3, fibrous.

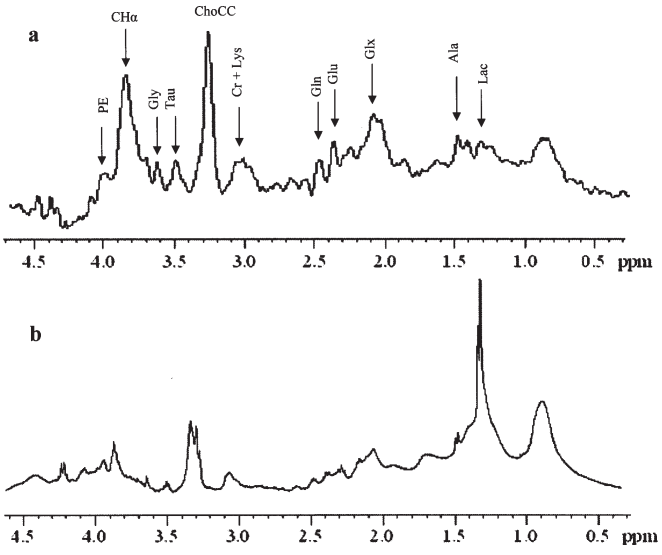

Figure 9. *In vivo* (a) (TE = 38 ms) and *ex vivo* (b) MR spectra of 5, meningothelial.

-CH_2-CH= moiety of mono- and poly-unsaturated fatty acids. The signals centered at 2.78 ppm are attributable to the methylenic protons between two double bonds (=C-CH_2-C=) in poly-unsaturated acids (linoleic and α-linolenic). The spectrum of sample 1 (meningothelial) is characterised by bonded amino acids and phospholipids, and by a large amount of triglycerides and represents an intermediate situation between that of sample 2 and 3.

Polyols. All spectra show the presence of mannitol (Man), which was given to the patients before surgery for cerebral decompression, in varying amounts. Man is identified by a characteristic group of signals in the region 3.4 ÷3.9 ppm, and through $^{1}H,^{13}C$ correlations [3.68, 3.88/63.3 ppm (CH_2OH); 3.76/71.3 ppm and 3.80/69.7 ppm] (Fig. 6).

The H-1 signals of α- and ß-glucose (Glc) (at 5.24 and 4.67 ppm, respectively) are clearly detected in samples 3 and 6. In addition, sample 3 displays resonances attributable to α-Glc-(1→4) units, embedded in small oligosaccharides. The two doublets at 5.41 and 5.39 ppm are due to H-1 of α-Glc-(1→4), as confirmed by the C-1 chemical shift at 100.2 ppm (35). Other signals due to α-Glc-(1→4) units are found by the inspection of the TOCSY and HSQC spectra (Fig. 6): H-1 protons correlate with H-2 protons at 3.64 and 3.55 (C-2 at 72.2 ppm), and with H-3 protons at 3.97 and 3.68 ppm (C-3 at 74.0 ppm). The pairs H-4/C-4 at 3.68/77.2 and at 3.43/70.0 ppm are attributable to central α-Glc-(1→4) units and the non-reducing terminal unit, respectively. The resonances of the reducing terminal unit are hidden under the signals of α- and ß-Glc and only the signal due to H-1 (4.66 ppm) of the reducing ß-Glc unit can be detected. The resonances of CH_2OH in Glc and α-Glc-(1→4) are found at 3.85/61.7 ppm. These data suggest the presence of oligosaccharides, probably maltotriose or maltotetraose. To our knowledge, it is the first time that these small sugars have been detected by MRS in human meningiomas.

Other minor signals due to Myo and scillo-inositol are found in all samples, whereas ribose signals, bonded to UMP and UDP nucleotides were detected, especially in samples 1 and 2.

Table III. Abundance of metabolites.[a]

Sample	Ala 1.48[b]	Glx 2.35+2.44[b]	Cr 3.04[b]	Cho 3.20[b]	ChoCC 3.20-3.23[b]	Tau 3.42[b]	Gly 3.56[b]	Ala/Cr	ChoCC/Cr
1	1	2.31	0.18	1.14	2.87	0.72	0.63	5.6	16.0
2	1	1.24	0.50	0.87	1.56	0.29	0.54	2.0	3.1
3	1	2.72	0.65	2.74	5.34	2.32	1.02	1.5	8.1
5	1	1.48	0.40	2.26	4.50	1.10	0.95	2.5	11.2
6	1	2.48	0.20	2.80	4.95	1.54	0.60	5.0	24.8

[a]The integral is evaluated with respect to that of Ala=1. [b]The chemical shift values denote the signals used for integration.

In vivo MR spectra. The *in vivo* MR spectra (TE=38 ms) of three different subtypes of meningioma, 3 (fibrous), 4 (oncocytic) and 5 (meningothelial), are reported in Fig. 7.

The three subtypes of meningioma are characterised by different metabolic profiles and on the basis of the analysis of the corresponding *ex vivo* spectra, it is possible to interpret the main features of each spectrum. The *in vivo* resonances at 0.9, 1.3, 2.1 and 2.8 ppm of sample 3 are mainly due to lipids and the broad signal around 2.1 ppm, besides triglycerides, receives a contribution from Glx, but not from NAA. Regarding the ChoCC at 3.2 ppm, it should be underlined that this signal, usually assigned in the *in vivo* spectrum to ChoCC, receives substantial contributions from Tau, Myo and PE, and minor ones from Arg and ß-Glc. Furthermore, in the *in vivo* spectrum the abundant signal at 3.4 ppm is recognizable due to Tau, and low signals at 3.0 ppm due to Cr and Lys.

A direct comparison between *in vivo* (TE=38 ms) and conventional (zgcppr) *ex vivo* spectra (after a suitable broadening processing) of sample 3 shows a close correspondence between the two profiles (Fig. 8).

The slight difference between the *in vivo* and the *ex vivo* signal at around 3.8 ppm is explainable by considering that while the *in vivo* signal receives contributions from PE and α-CH amino acids, the *ex vivo* shows additional contribution from Man.

The *in vivo* spectrum of sample 5 (meningothelial) in comparison with that of sample 3 (fibrous) (Fig. 7) is characterised by the lack of the resonances pertaining to triglycerides and by the presence of phospholipids and macromolecules. It is to be underlined that in the *in vivo* spectrum of 5, the signals due to Ala and Lac are well recognisable as doublets at 1.47 and 1.33 ppm, respectively.

A direct comparison between the *in vivo* (TE=38 ms) and the conventional (zgcppr) *ex vivo* spectra (after a suitable broadening processing) of sample 5 shows a good correspondence between the two profiles (Fig. 9), the only difference being the increased amount of Lac in the *ex vivo* spectrum.

The metabolic profile of *in vivo* MR spectrum of sample 4 (oncocytic; its *ex vivo* spectrum is not available) is between those of 3 and 5 and displays an increased amount of triglycerides with respect to 5. Other well-identified metabolites in samples 3 and 5 are marked on the corresponding spectra.

The *in vivo* spectra obtained with an echo time of 144 ms, and routinely used for diagnostic purposes, should be compared to the CPMG *ex vivo* ones, permitting evaluation of the ChoCC/Cr ratio. These ratios derived from *in vivo* measurements are 2.3, 7.9 and 9.3 for samples 2, 3 and 5, respectively, and are in good accordance with the *ex vivo* ones: 3.1, 8.0 and 11.0.

In conclusion, *ex vivo* HR-MAS MRS allowed us to make an accurate description of the metabolic profile of different meningiomas. By using 1D (composite pulse, water-suppressed spin-echo Carr-Purcell-Meiboom-Gill and diffusion-edited sequences) and 2D (COSY, TOCSY and HSQC) experiments, we were able to evidence the presence of several metabolites in different histological subtypes of meningioma. The HR-MAS results agree with the findings in several reports on the major metabolites (Ala, ChoCC, Glx, together with a marked decrease or absence of Cr) found in *in vitro* and *in vivo* MRS spectra of meningiomas (33,36-39). Whereas several *in vivo* studies on human meningiomas are well documented (1,2,24,31,40-42) only one report (43) exists on the ^{1}H HR-MAS MR spectrum of a meningioma in comparison with different brain tumors.

Our spectroscopic data, obtained from the six samples of meningiomas, confirmed the presence of the typical metabolites of these benign neoplasms and, at the same time, that meningiomas with different morphological characteristics have different metabolic profiles, particularly regarding macromolecules and lipids.

The *ex vivo* spectra, permitting a better understanding and interpretation of the *in vivo* MR spectra, show that the HR-MAS MRS technique is a complementary method to strongly support *in vivo* MR spectroscopy and increase its clinical potentiality.

Acknowledgements

The Fondazione Cassa di Risparmio di Modena is greatly acknowledged for the financial support given for the acquisition of the Bruker Avance400 Spectrometer and the Philips Intera 3 Tesla MR scanner. The Centro Interdipartimentale Grandi Strumenti of the University of Modena and Reggio Emilia and the Azienda Ospedaliero-Universitaria Policlinico di Modena are also greatly acknowledged. This work was supported by grants of Murst ex 60% to V.T.

References

1. Harting I, Hartmann M, Bonsanto MM, Sommer C and Sartor K: Characterization of necrotic meningioma using diffusion MRI, perfusion MRI, and MR spectroscopy: case report and review of the literature. Neuroradiology 46: 189-193, 2004.
2. Cho YD, Choi GH, Lee SP and Kim JK: 1H-MRS metabolic patterns for distinguishing between meningiomas and other brain tumors. Magn Reson Imag 21: 663-672, 2003.
3. Millis KK, Maas WE, Cory DG and Singer S: Gradient, high-resolution, magic-angle spinning nuclear magnetic resonance spectroscopy of human adipocyte tissue. Magn Reson Med 38: 399-403, 1997.
4. Cheng LL, Ma MJ, Becerra L, Ptak T, Tracey I, Lackner A and Gonzalez RG: Quantitative neuropathology by high resolution magic angle spinning proton magnetic resonance spectroscopy. Proc Natl Acad Sci USA 94: 6408-6413, 1997.
5. Beckonert OP, Nicholson JK and Lindon JC: High resolution magic angle spinning and MR spectroscopy of tumor tissues: Techniques and Applications. In: Nuclear Magnetic Resonance Spectroscopy in the Study of Neoplastic Tissues. Tosi R and Tugnoli V (eds). Nova Science Publisher Inc., New York, pp397-437, 2005.
6. Duarte IF, Stanley EG, Holmes E, Lindon JC, Gil AM, Tang H, Ferdinand R, McKee CG, Nicholson JK, Vilca-Melendez H, Heaton N and Murphy GM: Metabolic assessment of human liver transplants from biopsy samples at the donor and recipient stages using high-resolution magic angle spinning ^{1}H NMR spectroscopy. Anal Chem 77: 5570-5578, 2005.
7. Li W, Lee REB, Lee RE and Li J: Methods for acquisition and assignment of multidimensional high-resolution magic angle spinning NMR of whole cell bacteria. Anal Chem 77: 5785-5792, 2005.
8. Tugnoli V, Schenetti L, Mucci A, Nocetti L, Toraci C, Mavilla L, Basso G, Rovati R, Tavani F, Zunarelli E, Righi V and Tosi MR: A comparison between *in vivo* and *ex vivo* HR-MAS ^{1}H MR spectra of a pediatric posterior fossa lesion. Int J Mol Med 16: 301-307, 2005.

9. Martinez-Bisbal MC, Marti-Bonmati L, Piquer J, Revert A, Ferrer P, Llàcer JL, Piotto M, Assemat O and Celda B: ^{1}H and ^{13}C HR-MAS spectroscopy of intact biopsy samples *ex vivo* and *in vivo* ^{1}H MRS study of human high grade gliomas. NMR Biomed 17: 191-205, 2004.
10. Sitter B, Autti T, Tyynelae J, Sonnewald U, Bathen TF, Puranen J, Santavuori P, Haltia MJ, Paetau A, Polvikoski T, Gribbestad IS and Haekkinen AM: High-resolution magic angle spinning and 1H magnetic resonance spectroscopy reveal significantly altered neuronal metabolite profiles in CLN1 but not in CLN3. J Neurosci Res 77: 762-769, 2004.
11. Swanson MG, Vigneron DB, Tabatabai ZL, Males RG, Schmitt L, Carroll PR, James JK, Hurd RE and Kurhanewicz J: Proton HR-MAS spectroscopy and quantitative pathologic analysis of MRI/3D-MRSI-targeted postsurgical prostate tissues. Magn Reson Med 50: 944-954, 2003.
12. Sitter B, Bathen T, Hagen B, Arentz C, Skjeldestad FE and Gribbestad IS: Cervical cancer tissue characterized by high-resolution magic angle spinning MR spectroscopy. MAGMA 16: 174-181, 2004.
13. Kleihues P and Cavenee WK (eds): Pathology and Genetics. Tumours of the Nervous System. World Health Organization Classification of Tumours. IARC Press 1, 2000.
14. Roncaroli F, Riccioni L, Cerati M, Capella C, Calbucci F, Trevisan C and Eusebi V: Oncocytic meningioma. Am J Surg Pathol. 21: 375-382, 1997.
15. Bax A: A spatially selective composite 90º radiofrequency pulse. J Magn Reson 65: 142-145, 1985.
16. Meiboom S and Gill D: Modified spin-echo method for measuring nuclear relaxation time. Rev Sci Instrum 29: 688-691, 1958.
17. Wu D, Chen A and Johnson Jr CS: An improved diffusion-ordered spectroscopy experiment incorporating bipolar gradient pulses. Magn Reson Series A 115: 260-264, 1995.
18. Jeener J: Pulse pair techniques in high resolution NMR. Ampere International Summer School II, Basko Polje, Yugoslavia, 1971.
19. Aue WP, Bartholdi E and Ernst RR: Two-dimensional spectroscopy. Application to nuclear magnetic resonance. J Chem Phys 64: 2229-2246, 1976.
20. Braunschweiler L and Ernst RR: Coherence transfer by isotropic mixing: application to proton correlation spectroscopy. J Magn Reson 53: 521-528, 1983.
21. Bax A and Davis DG: MLEV-17-based two-dimensional homonuclear magnetization transfer spectroscopy. J Magn Reson 65: 355-360, 1985.
22. Bodenhausen G and Ruben DJ: Natural abundance nitrogen-15 NMR by enhanced eteronuclear spectroscopy. Chem Phys Lett 69: 185-189, 1980.
23. Liu MP, Beigelman L, Levy E, Handschumacher RE and Pizzorno G: Discrete roles of hepatocytes and non parenchymal cells in uridine catabolism as a component of uridine homeostasis. Am J Physiol 274 (Gastrointest Liver Physiol 37) G1018-G1023, 1998.
24. Opstad KS, Provencher SW, Bell BA, Griffiths JR and Howe FA: Detection of elevated glutathione in meningiomas by quantitative *in vivo* ^{1}H MRS. Magn Reson Med 49: 632-637, 2003.
25. Balendiran GK, Dabur R and Fraser D: The role of glutathione in cancer. Cell Biochem Funct 22: 343-352, 2004.
26. Locigno R and Castronovo V: Reduced glutathione system: Role in cancer development, prevention and treatment. Int J Oncol 19: 221-236, 2001.
27. Townsend DM and Tew KD: The role of glutathione-S-transferase in anti-cancer drug resistance. Oncogene 22: 7369-7375, 2003.
28. Wu G, Fang YZ, Yang S, Lupton JR and Turner ND: Glutathione metabolism and its implications for health. J Nutr 134: 489-492, 2004.
29. Huxtable RJ: Physiological actions of taurine. Physiol Rev 72: 101-163, 1992.
30. Dominy J, Eller S and Dawson Jr R: Building biosynthetic schools: Reviewing compartmentation of CNS taurine synthesis. Neurochem Res 29: 97-103, 2004.
31. Preul MC, Caramanos Z, Collins DL, Villemure JG, Leblanc R, Olivier A, Pokrupa R and Arnold DL: Accurate non invasive diagnosis of human brain tumors by using proton magnetic resonance spectroscopy. Nat Med 2: 323-325, 1996.
32. Florian CL, Preece NE, Bhakoo KK, Williams SR and Noble MD: Type-specific fingerprint of meningioma and meningeal cells by proton nuclear magnetic resonance spectroscopy. Cancer Res 55: 420-427, 1995.
33. Gill SS, Thomas DGT, Van Bruggen N, Gadian GD, Peden CJ, Bell JD, Cox IJ, Menon DK, Iles RA, Bryant DJ and Coutts GA: Proton NMR spectroscopy of intracranial tumors: *in vitro* and *in vivo* studies. J Comput Assist Tomogr 14: 497-504, 1990.
34. Richarz R and Wuthrich K: Carbon-13 NMR chemical shifts of the common amino acid residues measured in aqueous solutions of the linear tetrapeptides H-Gly-Gly-X-L-Ala-OH. Biopolymers 17: 2133-2141, 1978.
35. Degn P, Larsen KL, Duus JØ, Petersen BO and Zimmermann W: Two-step enzymatic synthesis of maltooligosaccharide esters. Carbohydr Res 329: 57-63, 2000.
36. Peeling J and Sutherland G: High-Resolution ^{1}H NMR spectroscopy studies of extracts of human cerebral neoplasms. Magn Reson Med 24: 123-136, 1992.
37. Kinoshita Y and Yokota A: Absolute concentrations of metabolites in human brain tumors using *in vitro* proton magnetic resonance spectroscopy. NMR Biomed 10: 2-12, 1997.
38. Tugnoli V, Tosi MR, Barbarella G, Ricci R, Leonardi M, Calbucci F and Bertoluzza A: Magnetic resonance spectroscopy study of low grade extra and intracerebral human neoplasms. Oncol Rep 5: 1199-1203, 1998.
39. Lehnhardt FG, Bock C, Rohn G, Ernestus RI and Hoehn M: Metabolic differences between primary and recurrent human brain tumors: a ^{1}H NMR spectroscopic investigation. NMR Biomed 18: 371-382, 2005.
40. Howe FA and Opstad KS: ^{1}H MR spectroscopy of brain tumours and masses. NMR Biomed 16: 123-131, 2003.
41. Majòs C, Alonso J, Aguilera C, Serralonga M, Coll S, Acebes JJ, Arùs C and Gili J: Utility of proton MR spectroscopy in the diagnosis of radiologically atypical intracranial meningiomas. Neuroradiology 45: 129-136, 2003.
42. Majòs C, Julià-Sapè M, Alonso J, Serralonga M, Aguilera C, Acebes JJ, Arùs C and Gili J: Brain tumor classification by proton MR spectroscopy: comparison of diagnostic accuracy at short and long TE. AJNR 25: 1696-1704, 2004.
43. Barton SJ, Howe FA, Tomlins AM, Cudlip SA, Nicholson JK, Bell BA and Griffith JR: Comparison of *in vivo* ^{1}H MRS of human brain tumors with ^{1}H HR-MAS spectroscopy of intact biopsy samples *in vitro*. MAGMA 8: 121-128, 1999.